Journal of the European Ceramic Society 22 (2002) 1095–1102

www.elsevier.com/locate/jeurceramsoc

Interactions between an ABS type leadless glaze and a biscuit fired bone china body during glost firing. Part I: preparation of experimental phases

Alpagut Kara[a,*], Ron Stevens[b]

[a]*Department of Ceramic Engineering, Anadolu University, Eskişehir, Turkey*
[b]*Department of Engineering and Applied Science, University of Bath, Bath, UK*

Received 16 February 2001; accepted 16 July 2001

Abstract

In this paper, part of an extended study, crystalline phases of a biscuit fired bone china body, namely anorthite and beta-tricalcium phosphate (β-TCP), were produced experimentally to be used in subsequent interface studies for simulation of the interactions during glost firing at different temperatures between an ABS type commercial leadless glaze and the individual phases originally present in the body. The research was undertaken based on the premise that bone china has been a product providing the greatest challenge in moving to a totally leadless glaze. High bulk density and low apparent porosity values were achieved from both the anorthite and β-TCP samples through the suitable heat treatments. The microstructural and chemical characteristics of the experimental phases were studied using X-ray diffraction (XRD), scanning (SEM), and transmission (TEM) electron microscopy techniques in combination with EDS analysis. The morphological and chemical similarity of the phases to those originally present in a biscuit fired bone china body was clearly demonstrated. This similarity supports the choice of the experimental material for the interface studies undertaken with these phases in the second part of the study.

Keywords: Anorthite; Bone china; $Ca_3(PO_4)_2$; Glaze; Interfaces

1. Introduction

The chemical and phase composition of a glaze tends to change during glost firing as a consequence of two main factors. The first, is the volatilisation of part of the glaze constituents from the surface. However, volatilisation is limited in high temperature glazes, which do not contain lead and boron. A further reason for the change in glaze composition is the interactions which occur at the glaze–body interface. As the glost firing approaches its peak temperature, the glaze becomes fluid and reacts with the underlying ceramic body. There is subsequent diffusion of chemical species from the body into the glaze and vice versa. This interdiffusion of ions can result in a change in the distribution of elements over the interface and the creation of new phases having different interface morphologies. The interactions between the glaze and the body can be characterised by determining the spatial distribution of the elements involved, by identifying any new phases that have formed, and determining the final morphology of the interface.

The glaze–body interactions which take place during glost firing depend on several variables.[1] These include the composition of the body and the glaze, the thickness of the glaze layer, the peak glost firing temperature and soaking time, the processing route (once or twice fired), whether or not the glaze is fritted and to what extent, the viscosity of the molten glaze and the mutual solubility of body and glaze components.

Glaze–body interactions during glost firing are of significance since they largely determine the physical, chemical and mechanical properties of the as-fired glaze such as craze resistance, strength, abrasion properties, chemical resistance, aesthetic appearance and maturing behaviour of the glaze, etc. For example; interaction layers can be formed, consisting of crystals, which may or may not be thermally compatible with either body or glaze and they would thus affect the overall strength of the system. Interaction layers, when in the glassy liquid state can also

* Corresponding author. Tel.: +90-222-3213550x6360, fax: +90-222-3239501.
E-mail address: akara@anadolu.edu.tr (A. Kara).

0955-2219/02/$ - see front matter
PII: S0955-2219(01)00419-8

be expected to have different viscosities and surface tensions and consequently to release bubbles in the system at very different rates. Because of this, the same glaze fired on different bodies can give quite different surface qualities. Furthermore, the chemical composition of the body is of significance in the manner in which it influences subsidiary glaze reactions, such as how it affects the bubble volume fraction, size and size distribution. A high quality gloss finish cannot be obtained if the glaze contains an excess of bubbles. The amount of free silica and its particle size, present at the glaze–body interface, also affects the glaze quality. Franklin[2] showed that the retention of larger bubbles was associated with the presence of coarse silica particles in the body. The bubble retention was considered to be due to a particular chemical relationship between the silica particle and the glaze, but the manner in which this interaction proceeds could not be explained.

Although glaze–body interactions have been studied by several authors using different techniques and their importance on many properties of the finished ware has been freely acknowledged, the topic has, on the whole, been treated only in a general manner. The most comprehensive work was by Roberts and Marshall,[3] who developed an apparatus for the study of glaze–body interactions by means of electrochemical measurements. The interfacial e.m.f values resulting from the contact of bone china, earthenware, their crystalline and vitreous phases and different glazes were measured over a range of temperatures and the results interpreted in terms of the reactions taking place. It was shown that reactions of a galvanic character could take place at the interface involving different ceramic phases in contact, with the molten glaze acting as an electrolyte. They related this interfacial e.m.f to the diffusion of ions from one phase to another, and this in turn was related to the solution of one phase in another. It was found that the mullite phase made the major contribution to the reactions as far as the earthenware composition was concerned, but in the case of bone china, it was the glassy phase. They employed an electron probe microanalyser (EPMA) to verify the results.

Roberts and Beech[4] had earlier discussed the theoretical influences of the glaze–body interactions on the properties of a biscuit fired bone china body. The composition and thermal expansion properties of the interaction layer were examined by means of synthetic mixtures and the separation of individual layers, sectioned from the body and glaze interface. The presence of an apatite phase, which was proposed to be the result of the reaction between the β-TCP constituent of the body with CaO from the glaze, was confirmed by XRD analysis. In order to support this proposal, further experiments were carried out with CaO free glazes. It was shown that there was no apatite formation in the interaction layer with this type of glaze.

In a recent study, Ichiko[5] investigated the relationship between the development of interaction layers between different glazes and a bone china body and mechanical properties by varying glost firing temperatures and soaking times. He found that the mechanical strength of bone china was indeed affected by the development of interaction layers, and tended to exhibit a high value when the coefficient of thermal expansion of the interaction layer was intermediate between those of the glaze and the body. In addition, hydroxyapatite was observed to be present in the interaction layers.

With the transition to leadless glaze systems, various leadless glaze compositions have emerged for use with a wide range of tableware body formulations such as earthenware, hotelware, and bone china. The main leadless glaze systems are advanced borosilicate systems (ABS), low and high bismuth glazes and zinc–strontium glazes.[6–8] However, work has yet to appear in the relevant literature concerning the interactions between these glazes and different tableware bodies during glost firing.

This part of the study was limited to the preparation of the crystalline phases of a typical biscuit fired bone china body in order that they might be used in the subsequent interface studies for simulating independently the interactions between an ABS type leadless glaze and the individual phases originally present in the body during glost firing at different temperatures. Such simulation is necessary since there is more than one phase present at the interface between the glaze layer and the underlying body at all times during glost firing and the degree of the interactions depends on the amount of each phase present in the body, apart from glaze composition and glost firing temperature. Bone china was particularly chosen on the premise that it has been a product providing the greatest challenge in moving to a totally leadless glaze. The most recent study on the biscuit firing of a bone china body and the formation and the chemistry of its constituent phases was carried out by Kara and Stevens.[9,10] They successfully demonstrated that β-TCP, anorthite and a negligible amount of quartz were the only crystalline phases, rather unevenly dispersed in a glassy matrix phase following firing at a peak temperature of 1245 °C for 1 h soaking. In addition, the glassy matrix phase was shown to have inhomogeneous distribution and varying chemistry. Thus, the present authors did not attempt to investigate the contribution of the glassy matrix phase to the interactions in this study.

2. Experimental

2.1. Material preparation

2.1.1. Bone China body

The same biscuit fired bone china body previously studied by Kara and Stevens[9,10] was chosen in order to

demonstrate the morphological and chemical similarity of the experimental crystalline phases to those originally present in the body. The details of sample preparation and firing regime were presented in these papers.

2.1.2. Anorthite

The dense anorthite pellets were made by solid-state reaction between New Zealand kaolin and ball milled calcium carbonate. The kaolin was supplied, in the powder form, by Goonvean Ceramics Materials Ltd (UK). New Zealand kaolin, or more precisely New Zealand halloysite, contains limited amounts of alkaline and alkaline-earth elements. The fine particle size enables this type of kaolin to be used extensively as a suspension agent in glaze preparations and the purity of the mineral ensures its inclusion in the product as a ceramic material for the production of porcelain and fine china. The low iron and titania content imparts exceptional whiteness and translucency to the fired ceramic ware. Table 1 shows the typical chemical composition of New Zealand kaolin.[11]

The calcium carbonate, ($CaCO_3$), powder was supplied by Prolabo (UK). It is Rectapur grade and has a purity minimum of 99%. Prior to mixing with the kaolin, it was ball-milled overnight, since it was considered that the particle size distribution of the $CaCO_3$ would affect the sintering process. The milling was carried out in isopropanol with zirconia ball media. Following the milling, particle size distribution measurement was carried on the powder using a laser diffraction particle size analyser, (Malvern Instruments Ltd. UK).

The kaolin and the ball-milled $CaCO_3$ were mixed such that the ratio of the dehydrated kaolin:CaO was ~80:20 (wt.%). The mixing was achieved in a ball-mill in isopropanol using zirconia balls. After drying, 1 g of the mixed powders was uniaxially pre-pressed in a stainless steel die at a low pressure to form a pellet of 20 mm in diameter. Following the uniaxial pressing, the pellets were cold isostatically pressed at a pressure of 100 MPa. The firing took place in an electric chamber furnace (Model: CWF 13/13, Carbolite, UK). During the firing, the pellets were supported by alumina grog spread on alumina plates.

Table 1
Typical chemical analysis of New Zealand kaolin[11]

Oxide	Wt.%
SiO_2	50.4
Al_2O_3	35.5
Fe_2O_3	0.25
TiO_2	0.05
CaO	Trace
MgO	Trace
K_2O	Trace
Na_2O	Trace
LOI	13.8

2.1.3. β-Tricalcium phosphate (β-TCP)

Tricalcium phosphate powder, with the composition $Ca_3(PO_4)_2$, supplied by Prolabo (UK), was used as a starting material for producing dense β-TCP pellets. The calcium content of the powder was reported by the supplier to be 35.5%. First, the as-received TCP powder was uniaxially pressed in a 20 mm stainless steel at a low pressure. The pellets were further cold isostatically pressed at a pressure of 200 MPa. The firing was achieved in the same electric chamber furnace.

2.2. Techniques

The bulk density and apparent porosity of the experimental phases were determined using the Archimedes' method with the theoretical density of 2.76 g/cm^3 for anorthite and 3.07 g/cm^3 for β-TCP respectively. The density of the fired β-TCP discs were, however, measured using ethanol rather than distilled water, to avoid any hydration effect.

X-ray diffraction (XRD) analyses were carried out using a Philips PW 1710 based diffractometer with a 40 kV generator voltage and a 25 mA current. The scans were made over a range of 2θ values of 5–80° with data acquisition occurring for 1.0 s, at intervals of 0.02°.

Both chemical and thermal etching techniques were employed to delineate the microstructure. Thermal etching of the experimental β-TCP was carried out in an electric chamber furnace. Etching of the experimental anorthite was done chemically in hydrofluoric acid (HF) solution.

A Jeol JSM-6310 analytical scanning electron microscope (SEM) fitted with an Oxford Instruments AN 10/85 Link microanalysis system was used to examine and analyse the polished and the etched surfaces of the representative samples.

TEM studies were performed using a Jeol 200 kV analytical electron microscope in order to investigate in greater detail the morphology of the experimental anorthite and β-TCP. All images were recorded using a 200 kV incident beam.

3. Results and discussion

3.1. Experimental anorthite

Following different firing trials at various sintering temperatures, the pellets fired at 1200°C for 1 h appeared to be the optimum samples from the observations of density, porosity and XRD measurements. The heating and the cooling rates were 1.7 and 3.3°C/min respectively. As can be seen from Table 2, a relative density of ~91%, with almost zero apparent porosity was achieved from the pellets by means of this heat treatment. These values are close to those which Kobayashi and Kato[12] obtained using $CaCO_3$ powder with a mean particle size

of 2.5 μm, at the same sintering temperature. The mean particle size of the ground $CaCO_3$ employed in this study was about 2.3 μm. The sintered pellets were white, and did not show any discoloration. A degree of translucency, which can be attributed to the fine grain size and low porosity, was noticeable.

Table 2
The physical properties of the experimental anorthite pellets

Property	Anorthite
Bulk density (g/cm^3)	2.50
Apparent porosity (%)	$\leqslant$0.5
Theoretical density (g/cm^3)	2.76
Relative density (%)	$\sim$91

XRD examination of the experimental anorthite pellets sintered at 1200 °C revealed only one crystalline phase, triclinic anorthite. A typical XRD spectrum is given in Fig. 1. Note that the spectrum has been normalised to the highest maximum intensity peak. The observed peaks in the sintered material coincide with the triclinic anorthite standard (JCPDS-ICDD No: 41-1486). The XRD spectrum of the experimental anorthite was compared with that of the biscuit fired bone china body. As can be seen

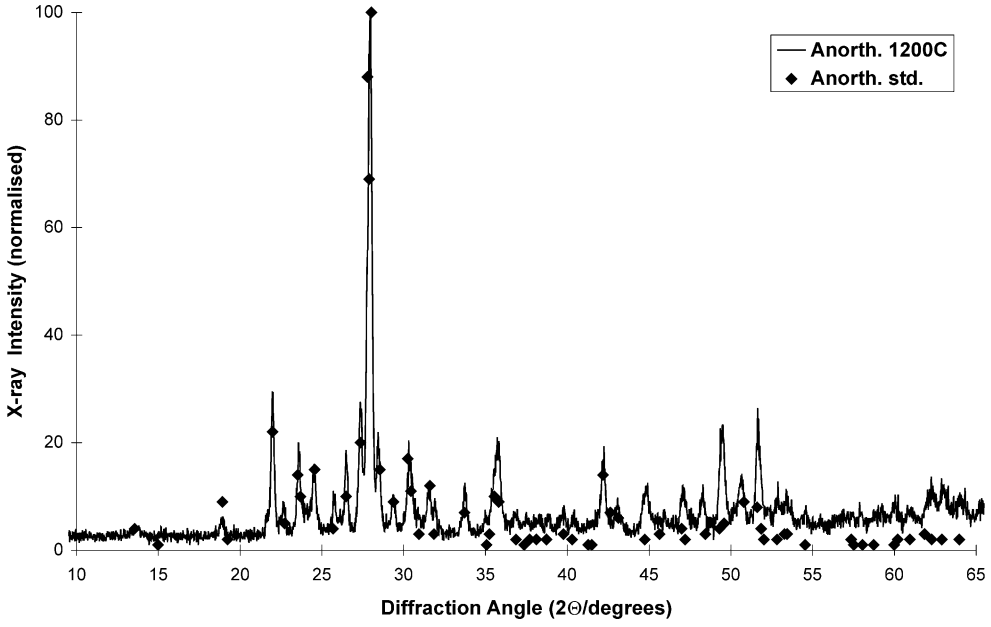

Fig. 1. A comparison of the XRD spectrum of the experimental anorthite.with the triclinic anorthite standard (JCPDS-ICDD No. 41-1486).

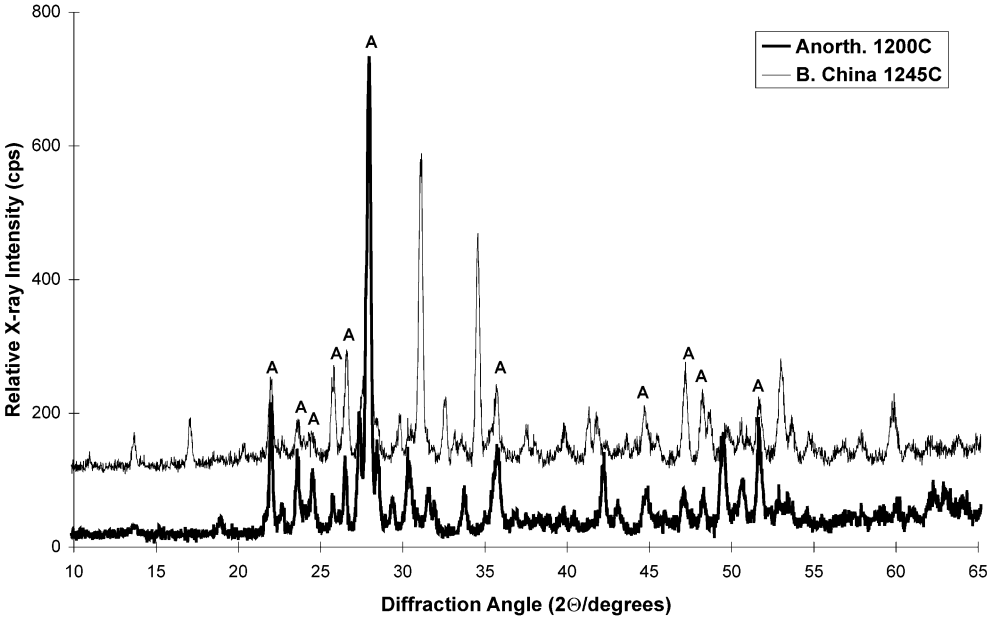

Fig. 2. A comparison of the XRD spectrum of the experimental anorthite with that of the biscuit fired bone china body (A: anorthite).

from Fig. 2, there is a good agreement between the major peaks from the experimental anorthite synthesised by solid-state reaction and the peaks from the anorthite phase originally present in the body.

SEM examination of the polished surfaces of the experimental anorthite pellets after etching with 1% HF solution for 60 s showed that the microstructure is composed of a fine grained matrix of crystals. Fig. 3 illustrates a typical secondary electron (SE) image of the anorthite microstructure where elongated, lath-like grains, with lengths ranging from 1 to 2 μm are randomly oriented with respect to each other. There are also large pores visible in the image and small pores between the grains. EDS analyses were carried out on the polished surfaces prior to etching in order to confirm the earlier XRD results. Fig. 4 gives such a spectrum showing the presence only of the elements Al, Si, Ca and O in the microstructure.

Fig. 5 illustrates a typical bright field TEM image of the microstructure. As can be seen, it exhibits elongated, lath-like anorthite crystals with interlocking grain boundaries. Another feature worth noting is the abundance of twinning and planar defects. Anorthite is the lime-rich end member of the plagioclase feldspar solid solution series; such twinning has been reported to be common in plagioclase minerals.[13]

3.2. Experimental β-tricalcium phosphate (β-TCP)

Following a series of firing trials over a range of different sintering temperatures, based on measurements of density, porosity and XRD, the pellets fired at 1140 °C for a soaking time of 6 hours appeared to give the best results. The heating and cooling rates were 1.3 °C/min. Table 3 lists the physical properties obtained as a result of this heat treatment. A relative density of 97% with almost zero apparent porosity was achieved indicating that sintering was virtually complete at this temperature. The sintered pellets were white, and did not show any discoloration. The pellets also showed a high degree of translucency, indicative of an almost pore free microstructure.

XRD examination of the experimental TCP pellets sintered at 1140 °C revealed the presence of only one crystalline phase, β-TCP. Fig. 6 shows such a spectrum. Note that the spectrum has been normalised to its maximum intensity peak. The observed peaks from the experimental β-TCP correlate closely with the pure β-TCP standard (JCPDS-ICDD No:09-169). In Fig. 7, The XRD spectrum of the experimental β-TCP was compared with

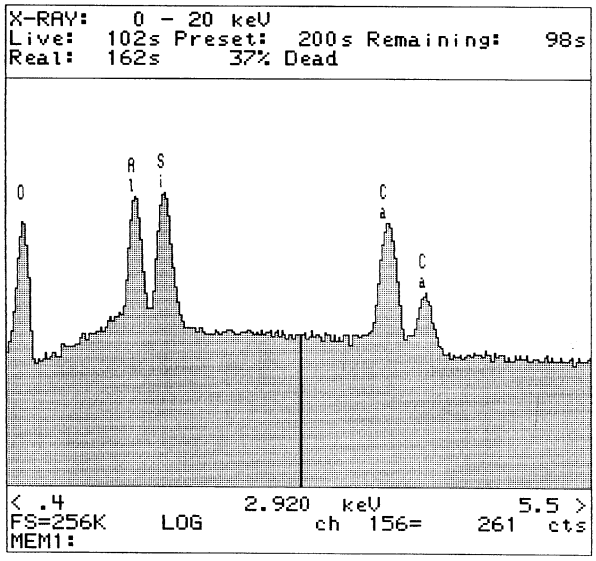

Fig. 4. A typical EDS spectrum of the experimental anorthite.

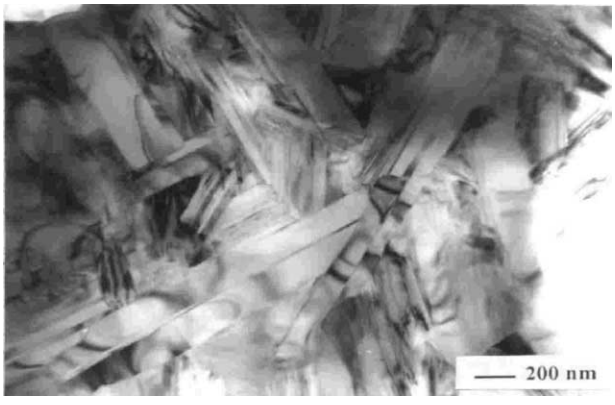

Fig. 5. A typical bright-field TEM image of the microstructure of the experimental anorthite.

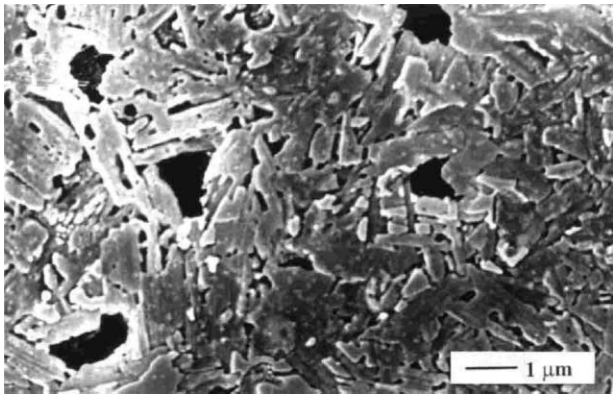

Fig. 3. A typical SE Image of the microstructure of the experimental anorthite (polished and etched surface).

Table 3
The physical properties of the experimental β-TCP pellets

Property	β-TCP
Bulk density (g/cm^3)	2.98
Apparent porosity (%)	⩽0.5
Theoretical density (g/cm^3)	3.07
Relative density (%)	~97

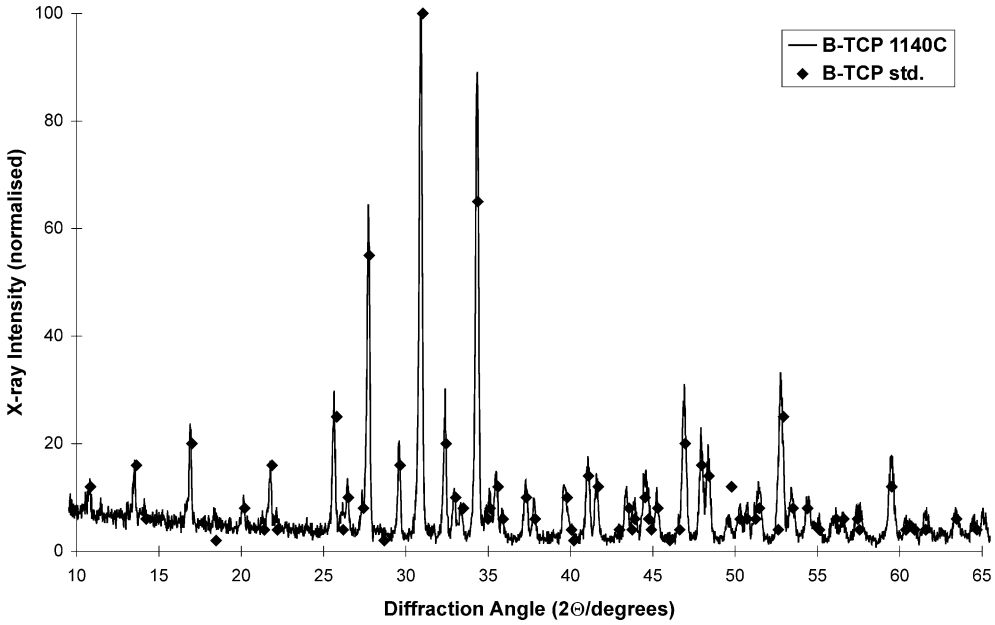

Fig. 6. A comparison of the XRD spectrum of the experimental β-TCP with the β-TCP standard.

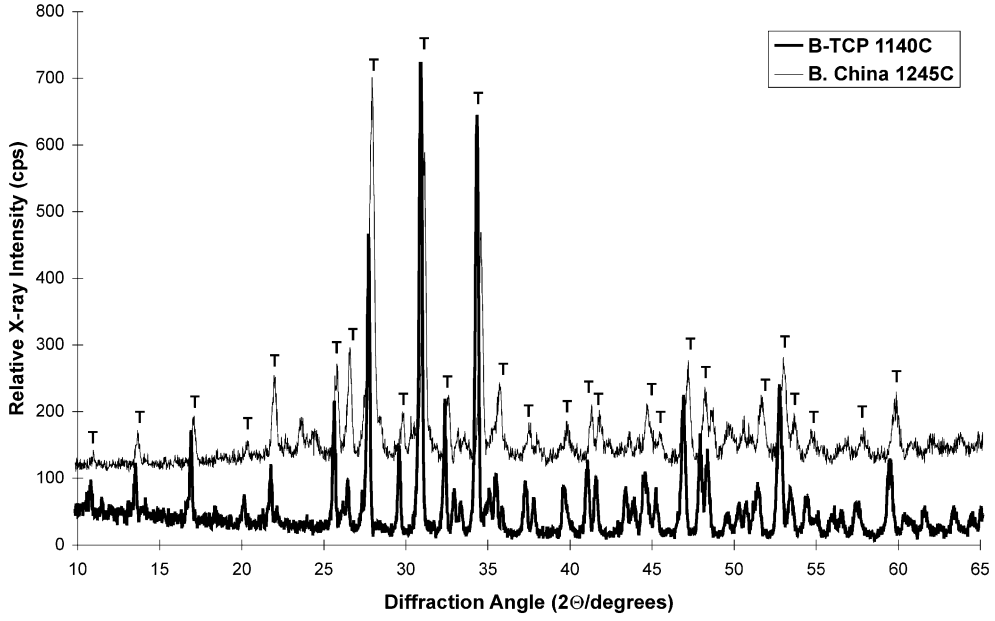

Fig. 7. A comparison of the XRD spectrum of the experimental β-TCP with that of the biscuit fired bone china body.

that of the biscuit fired bone china body. It was found that there is a good agreement between the two.

SEM examination of the polished surfaces of the experimental β-TCP pellets after the thermal etching at 1100 °C for 1 h clearly revealed the microstructure. Fig. 8 shows a typical SE image of the etched β-TCP microstructure. The individual grains and a few isolated pores at the grain boundaries are visible at this magnification. No secondary phase can be observed. The grains are generally small with an average grain size of 1.4 μm, with some larger grains present, due to grain growth. EDS analyses were carried out on the polished surfaces of the unetched specimens in order to confirm the presence of β-TCP as determined by XRD. Fig. 9 is such a spectrum showing the presence only of the elements P, Ca and O in the microstructure.

A typical bright field TEM image of the experimental β-TCP microstructure is shown in Fig. 10. As can be seen, there is no indication of a secondary phase or pores at the grain boundaries. Another feature of the micrograph is the presence of bend contours in the grains due to localised elastic strain.

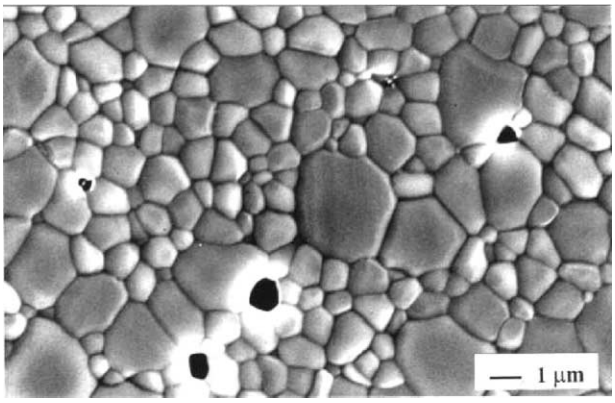

Fig. 8. A typical SEI image of the microstructure of the experimental β-TCP (polished and etched surface).

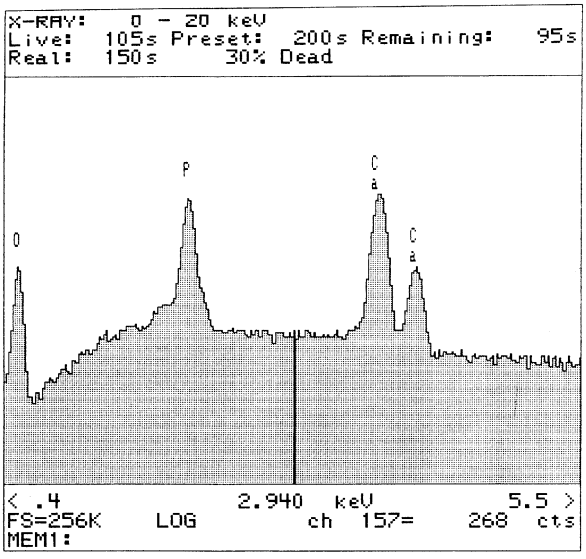

Fig. 9. A typical EDS spectrum of the experimental β-TCP.

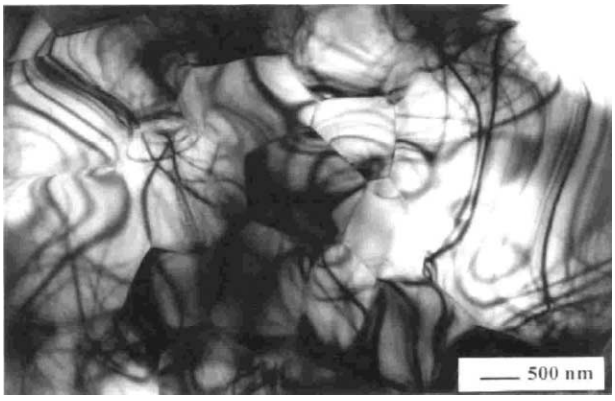

Fig. 10. A typical bright-field TEM image of the microstructure of the experimental β-TCP.

4. Conclusions

Dense anorthite pellets with almost zero apparent porosity have been successfully synthesised from relatively pure NZ kaolin and ground $CaCO_3$. As mentioned above, using a fine kaolin and controlling the particle size of $CaCO_3$ is important in order to obtain high density polycrystalline anorthite ceramics, particularly at low sintering temperatures. The mean particle size of the ground $CaCO_3$ used in this study was approximately 2.3 μm, and the resultant bulk density and the apparent porosity values of the anorthite pellets were found to be close to the data reported in the literature, this having been fabricated with a similar mean particle size. Achieving high bulk density and low apparent porosity was important, otherwise simulation of the interactions between the leadless glaze and the experimental anorthite during glost firing would have been difficult, owing to absorption of the glaze into the anorthite.

XRD analysis on the anorthite pellets showed that the main crystalline phase was triclinic anorthite. When the XRD spectrum of the experimental anorthite is compared with that of the biscuit fired bone china body, the anorthite peaks from the both materials were found to coincide, establishing their crystallographic compatibility. This finding supports the validity of the experimental material for the interaction studies. Moreover, SEM and TEM studies revealed that the microstructure of the experimental anorthite consists of elongated lath-like crystals with extensive twinning and planar defects. Similar structural features were also observed in the anorthite crystals present in the biscuit fired bone china body, previously examined by Kara and Stevens.[9,10]

A high bulk density and low apparent porosity of the sintered β-TCP pellets was also achieved on sintering a commercial powder. XRD analysis of the samples indicated that the only crystalline phase present was β-TCP, with identical structure to the bone china component. This supports the choice of the experimental material for the interaction studies. The microstructure of the experimental β-TCP was also characterised by SEM and TEM and shown to consist solely of crystalline grains with no indication of any secondary phase.

Acknowledgements

The authors would like to thank the Anadolu University (Turkey) for the provision of a scholarship.

References

1. Parmelee, C. W., *Ceramic Glazes*, 3rd ed. Cahners Books, Boston, 1973 (revised by C.G. Harman).
2. Franklin, C. E. L., The maturing behaviour of glazes II. The effect of the ceramic body. *Trans. Br. Ceram. Soc.*, 1966, **65**, 277–287.
3. Roberts, W. and Marshall, K., Glaze–body reactions: electrochemical studies. *Trans. Br. Ceram. Soc.*, 1970, **69**(6), 221–241.
4. Roberts, G. J. and Beech, D. G., Glaze–body relationship in bone china. Research Paper No. 433, *Br. Ceram. Res. Assoc.*, 1959.

5. Ichiko, T., A consideration about the glazing to the bone china. *J. Ceram. Soc. Jpn., Int. Ed.*, 1994, **102**(5), 473–477.
6. Cubbon, R. C. P., Consumer and environmental pressures on the use of lead glazes and colours. *Interceram.*, 1994, **43**(4), 240–242.
7. Alsop, S., Development of unleaded glazes for ceramic tableware. *Br. Ceram. Trans.*, 1994, **93**(2), 77–79.
8. Jackson, P. R., unleaded glazes and colours for tableware—an update. *Br. Ceram. Trans.*, 1995, **94**(4), 171–173.
9. Kara, A. and Stevens, R., Characterisation of biscuit fired bone china body microstructure, I. XRD and SEM of crystalline phases. *J. Eur. Cer. Soc.*, 2002, **22**(5), 731–736.
10. Kara, A. and Stevens, R., Characterisation of biscuit fired bone china body microstructure, II. Transmission electron microscopy (TEM) of glassy matrix. *J. Eur. Ceram. Soc.*, 2002, **22**(5), 737–743.
11. *Information Booklet*. New Zealand China Clays Ltd., Auckland, New Zealand.
12. Kobayashi, Y. and Kato, E., Low-temperature fabrication of anorthite ceramics. *J. Am. Ceram. Soc.*, 1994, **77**(3), 1994, 833–834.
13. Deer, W. A., Howie, R. A. and Zussman, J., *An Introduction to the Rock-Forming Minerals,* 6th imp. Longman Group, London, 1972.